Selective electrochemical detection of 2,4,6-trinitrotoluene (TNT) in water based on poly(styrene-co-acrylic acid) PSA/SiO$_2$/Fe$_3$O$_4$/AuNPs/lignin-modified glassy carbon electrode

Khaled A. Mahmoud, Ahmed Abdel-Wahab and Mohammed Zourob

ABSTRACT

A new versatile electrochemical sensor based on poly(styrene-co-acrylic acid) PSA/SiO$_2$/Fe$_3$O$_4$/AuNPs/lignin (L-MMS) modified glassy carbon electrode (GCE) was developed for the selective detection of trace trinitrotoluene (TNT) from aqueous media with high sensitivity. The fabricated magnetic microspheres were characterized by transmission electron microscopy (TEM), energy-dispersive X-ray spectroscopy (EDS), and X-ray photoelectron spectroscopy (XPS). L-MMS films were cast on the GCE surface to fabricate the TNT sensing electrode. The limit of detection (LOD) of TNT determined by the amperometric i-t curve reached 35 pM. The lignin film and well packed Fe$_3$O$_4$/AuNPs facilitated the pre-concentration of trace TNT on the electrode surface resulting in a fast amperometric response of 3 seconds near the detection limit. The high sensitivity and excellent catalytic activity of the modified electrode could be attributed to the lignin layer and highly packed Fe$_3$O$_4$/AuNPs on the electrode surface. The total recovery of TNT from tapwater and seawater matrices was 98% and 96%, respectively. The electrode film was highly stable after five repeated adsorption/desorption cycles. The new electrochemical sensing scheme provides a highly selective, sensitive and versatile assay for the in-$situ$ detection of TNT in complex water media.

Key words | lignin, magnetic nanoparticles, TNT, water treatment electrochemical detection

Khaled A. Mahmoud (corresponding author)
Qatar Environment and Energy Research Institute (QEERI),
Qatar Foundation, P.O. Box 5825,
Doha, Qatar
and
Hamad bin Khalifa University, P.O. Box 5825,
Education City,
Doha, Qatar
E-mail: kmahmoud@qf.org.qa

Ahmed Abdel-Wahab
Chemical Engineering Department,
Texas A&M University at Qatar,
Doha, Qatar

Mohammed Zourob
Centre Énergie, Matériaux et Télécommunications (ÉMT),
1650, boulevard Lionel-Boulet Varennes,
Québec, J3X 1S2, Canada
and
Center of Biomedical Engineering,
Cranfield University,
Vincent Building, Cranfield,
Bedfordshire, MK43 0AL, UK

INTRODUCTION

Water security is one of the most persistent issues due to the inadequate access to clean water and sanitation in many regions worldwide especially in third world countries. Also, environmental, health, and potential security concerns, including anti-terrorism, have generated high demands for portable, rapid, sensitive, and low cost detection of threatening contaminations in soil effluents, ground and surface waters. Nitroaromatic explosives, including 2,4,6-trinitrotoluene (TNT), have contaminated soils and aquifers worldwide because of their extensive utilization in military activities and improper waste management (McQuade *et al.* 2000; Thomas *et al.* 2007; Tenhaeff *et al.* 2010; Zhou *et al.* 2011). Due to their mutagenic and toxic properties, the presence of TNT in surrounding soils, waterways, and reservoirs must be monitored at ultratrace levels to mitigate the contamination risk. Among widely employed methods for detecting trace TNT (Caygill *et al.* 2012), electrochemical detection

methods are attractive because of the inherent redox activity of TNT and the portability of the electrochemical sensors (Blue *et al.* 2013; O'Mahony & Wang 2013). Surface modification of electrodes has been used to enhance the sensitivity and selectivity of electrochemical measurement including functionalized graphene (Tang *et al.* 2010; Lu *et al.* 2011), mesoporous SiO$_2$ (Zhang *et al.* 2006), AgNPs (Maduraiveeran & Ramaraj 2009; Chen *et al.* 2012), metal nanoparticles/carbon nanotubes (Hrapovic *et al.* 2006) and TiO$_2$ (Filanovsky *et al.* 2007). Among these nanostructures, noble nanoparticles such as AuNPs and AgNPs can provide a facile and versatile electrode surface with excellent electron transfer kinetics and a high signal to noise ratio (Li *et al.* 2010; Liu *et al.* 2011). An electrochemical sensor was established as a fast and inexpensive analytical alternative for on-site monitoring of nitroaromatic explosives in groundwater, including TNT, using a carbon fibre electrode (Fu *et al.* 2005). The method

was attractive because it can be integrated within a microfluidic platform for simultaneous sample handling and processing. A recent report has demonstrated that lignin-modified magnetic microspheres (L-MMS) can act as sensitive surface enhanced Raman (SERS) substrate for the selective detection of TNT from soil samples below 1×10^{-8} μg/g (Mahmoud & Zourob 2013). The urge for more cost-effective methods for on-site detection of explosives has led us to develop a new electrochemical sensing material comprising (polystyrene-co-acrylic acid) PSA/SiO$_2$ microsphere modified with highly packed Fe$_3$O$_4$/AuNPs and a lignin film coated on the glassy carbon electrode (GCE) for the ultra-trace detection of TNT. The modified electrode will be used for the ultrasensitive detection of TNT from water samples using voltammetric and amperometric electrochemical detection methods. Well-packed Fe$_3$O$_4$/AuNPs together with lignin coating is adopted as an excellent magnetic collector for pre-concentration of trace TNT in contaminated waters for subsequent electrochemical detection.

MATERIALS AND METHODS

Materials

Ferric chloride (FeCl$_3$·6H$_2$O), ferrous chloride (FeCl$_2$·4H$_2$O), sodium chloride (NaCl), triethylamine, hydrogen tetrachloroaurate(III) hydrate (99.9%), alkaline lignin, potassium persulfate (PPS), toluene, anhydrous ethanol, thioctic acid (Thc), aqueous ammonia (NH$_3$·H$_2$O, 28%), 2-(N-morpholino)ethanesulfonic acid (MES), N-Hydroxysuccinimide (NHS), N-(3-dimethylaminopropyl)-N'-ethylcarbodiimide (EDC), tetraethoxysilane (TEOS > 98%), and 3-aminopropyltriethoxysilane (APTES), were obtained from Sigma-Aldrich. 2,4,6-Trinitrotoluene (TNT), 2,4-dinitrotoluene (DNT), and dinitrobenzene (DNB) (1000 μg/mL) were obtained from Cerilliant Corporation, Texas.

Characterization tools

The size and morphology of the nanoparticles were examined by field emission transmission electron microscope (TEM) using a Philips CM200 microscope operating at 200 kV. Ten microliters of a dilute solution containing the nanoparticles was drop-casted on a carbon-coated copper grid (400 mesh) and dried under ambient conditions. EDX (Oxford) has software with a database of reference spectra for elemental analysis, compositional nano-analysis and mapping. The magnetic properties of the composite were investigated using a vibrating sampling magnetometer (VSM) 7,307 (Lakeshore Cryotronic, Westerville, Ohio). Electrochemical measurements were performed with a CHI workstation 760D (CH instruments, Austin, Texas). Glassy carbon electrodes (d = 2 mm) were pre-polished to a mirror finish with 1.0 and 0.3 μm alumina slurries and then rinsed with Milli-Q water, followed by electrochemical polishing in 0.5M H$_2$SO$_4$ by repeated cycling (0.15–1.0 V, scan rate 50 mVs^{-1}) until a stable voltammogram was obtained.

Preparation of PSA/SiO$_2$/Fe$_3$O$_4$/AuNPs microspheres (magnetic microspheres; MMS)

The PSA/SiO$_2$ was synthesized with an average diameter of 600 nm following the detailed procedure described elsewhere (Li et al. 2011; Mahmoud & Zourob 2013). The PSA/SiO$_2$/Fe$_3$O$_4$ microspheres were prepared according to the common co-precipitation method as described elsewhere with slight modification (Mahmoud & Zourob 2013). Briefly, FeCl$_3$·6H$_2$O (6.5 mg/mL) and FeCl$_2$·4H$_2$O (3.2 mg/mL) were mixed in 1% PSA/SiO$_2$ aqueous suspension. The suspension was vigorously stirred under nitrogen for 30 minutes. prior to the dropwise addition of ammonium hydroxide (0.65 mL, 28%). After heating at 80 °C for 2 hours, the resulting black precipitate was purified by three washing cycles with water/ethanol and was recovered by magnetic separation. The obtained PSA/SiO$_2$/Fe$_3$O$_4$ nanoparticles were then suspended in water to a final concentration (23 mg/mL, 4 mL) prior to the addition of HAuCl$_4$ (3.9 mg/mL, 1.6 mL) solution containing β-cyclodextrin (2.2 mg/mL, 2 mL). Ice-cold NaBH$_4$ (20 μL, 0.1 M) was then added dropwise to the slowly mixing solution until a stable reddish black colloid was obtained. The obtained PSA/SiO$_2$/Fe$_3$O$_4$/AuNPs colloid was purified by magnetic separation and washed (with water-ethanol) three times to remove any unbound AuNPs.

Preparation of lignin modified PSA/SiO$_2$/Fe$_3$O$_4$/AuNPs (L-MMS)

The PSA/SiO$_2$/Fe$_3$O$_4$/AuNPs was modified with lignin using a three step method. First, carboxylic acid groups were introduced to the PSA/SiO$_2$/Fe$_3$O$_4$/AuNPs by coupling Thc (1.5 mg/mL) to the AuNP surface via Au-S bonding. Second, aminated lignin was prepared by reacting lignin (100 mg) with epichlorohydrin (55 mg/g lignin) in 1 M NaOH for 2 hours at 60 °C to introduce the epoxy groups onto the lignin surface, followed by heating with 50% (w/v) NaOH, 29.4% NH$_4$OH (5 mL/g lignin) and maintaining the pH at 12 for 2

hours at 60 °C. The suspension was then neutralized with HCl (1 mL, 1 M) and the resulting (brown) precipitate was washed with water three times.

Third, aminated lignin was re-suspended in water and conjugated onto the carboxylated magnetic nanocomposite surface using a typical carbodiimide coupling protocol. In brief, 10 mM EDC and 20 mM NHS were added to PSA/SiO_2/Fe_3O_4/AuNPs/Thc (20 mg/mL) suspended in 0.05 M MES and 0.5 M NaCl buffer, pH 5.7 (5 mL). The suspension was stirred for 2 hours at room temperature. The activated MMS conjugate (5 mL, 50 mg) was recovered by magnetic separation and transferred to another vial containing aminated lignin (10 mg/ml) and triethylamine (pH 9, room temperature). The reaction was allowed to stir for 12 hours, the samples were then separated with a magnet and subjected to three washing cycles (water/methanol). The produced L-MMS was suspended in ethanol and was kept refrigerated for the electrochemical measurements.

Electrode modification and electrochemical detection experiments

To modify the glassy carbon electrode (GCE), a drop of a well dispersed ethanol suspension of L-MMS (20 μL, 1 mg/ml) was cast directly onto the surface of the electrode and the solvent was allowed to evaporate to form a stable film. The supporting electrolyte was purged with nitrogen gas prior to each experiment. The modified electrode was placed in an electrochemical cell containing 0.5 M NaCl solution as supporting electrolyte. The three-electrode electrochemical cell consisted of the modified GC working electrode, a Pt wire counter electrode and an Ag/AgCl (3 M NaCl) reference electrode (Bioanalytical Systems, West Lafayette, Indiana). Increasing concentrations of TNT were spiked into the electrolyte solution and the electrode was kept in contact with the stirred solution for 1 minute. prior to each run. The potential was scanned linearly between (−1.2 to 0) V, at 100 mVs^{-1}.

TNT pre-concentration and electrochemical assay

Solutions of fresh and seawater samples spiked with TNT were prepared in triplicate to give 1 μM concentrations of standard analytical reference TNT. Tapwater samples were collected from the municipal water of Doha (Qatar), and seawater was collected from the Arabian Gulf near Doha (Qatar). Samples were refrigerated immediately after collection for further use. Tapwater and seawater measured salinity were 430 ppm and 38,000 ppm, respectively.

Seawater was filtered with 0.2 μm nylon membrane prior to each experiment. Tapwater was used without further purification. TNT spiked water samples (1 mL, 1 μM) were shaken with 1 mg of L-MMS in 1.5 mL Eppendorf tube for 15 minutes at room temperature. The magnetic microspheres were then separated from the solution with a strong magnet, washed three times with deionized water, and finally re-suspended in ethanol (300 μL) in the same container. The collected magnetic microspheres were then drop-casted on per-polished GCE and allowed to dry to form a stable film for the electrochemical detection following the same protocol described above.

RESULTS AND DISCUSSION

Synthesis and characterization of L-MMS

Figure 1 describes the fabrication steps of L-MMS. The PSA/SiO_2 was synthesized as described elsewhere (Li *et al.* 2011). The Fe_3O_4NPs were formed on the surface of PSA/SiO_2 using the typical co-precipitation of $FeCl_3 \cdot 6H_2O$ and $FeCl_2 \cdot 4H_2O$ by ammonium hydroxide. AuNPs was grafted onto the surface of PSA/SiO_2/Fe_3O_4 using the modified Stöber method (Stöber *et al.* 1968). Thioctic acid (Thc) was used to introduce terminal carboxylic acid groups onto the surface of the AuNPs. Finally, aminated lignin was covalently attached to the surface of MMS using a two-step carbodiimide coupling protocol to impart high selectivity to the substrate due to the proven affinity of lignin towards TNT (Zhang *et al.* 2011). An initial lignin concentration of 60 mM was used to give the optimum surface coverage on MMS (Mahmoud & Zourob 2013). The stable and uniform dispersion of Fe_3O_4NPs and AuNPs on PSA/SiO_2 microspheres (600 nm) was then confirmed by the HRTEM as shown in Figure 2(a). AuNPs (3–7 nm in diameter) appeared to be darker than the 10–20 nm Fe_3O_4NPs as observed in the HRTEM micrograph (Figure 2(b)) due to the higher electron density of Au as compared with Fe_3O_4 (Robinson *et al.* 2010). The elemental composition was determined by energy-dispersive X-ray spectroscopy (EDS) as described in Figure 2(c). The metallic Fe represented by 0.75, 6.5, and 7 KeV signals confirmed the presence of Fe_3O_4NPs. The peaks at 2, 9.5 and 11.5 MeV represent AuNPs. The XPS pattern of the L-MMS showed well defined Fe binding energies for Fe2p$_{3/2}$ at 711 eV and Fe2p$_{1/2}$ at 724.4 eV due to the coexistence of Fe^{+2} and Fe^{+3} ions which are comparable to the literature values (Prakash *et al.* 2007). After lignin modification, a shoulder
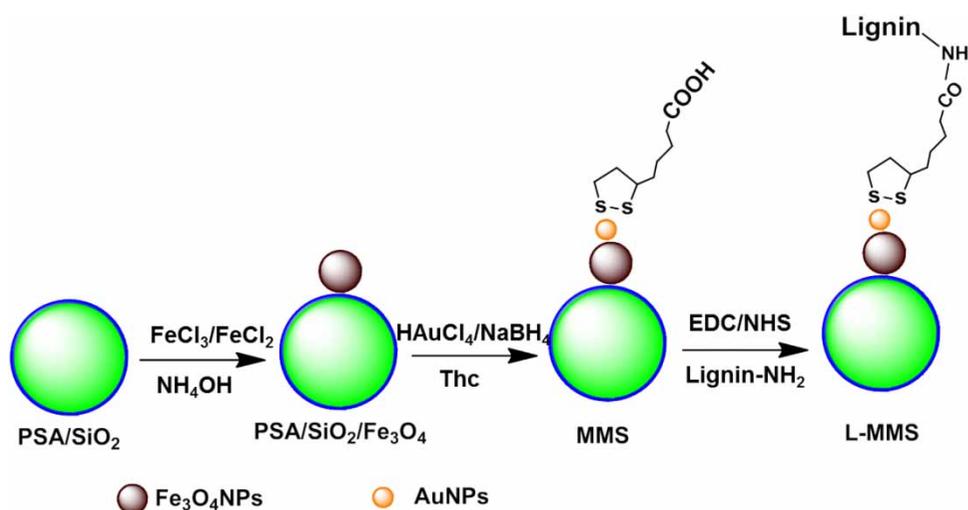
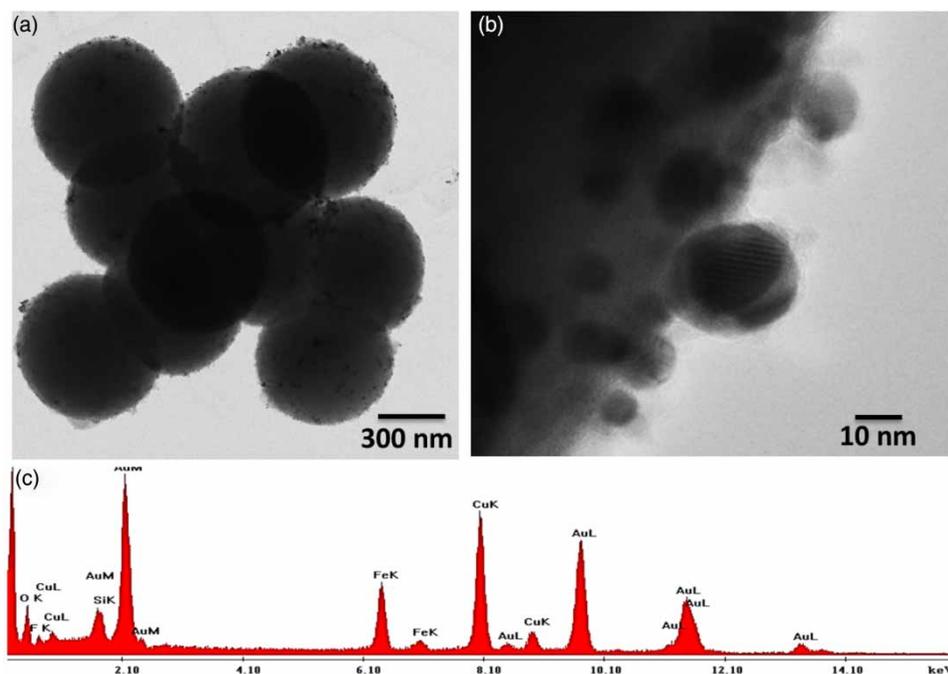**Figure 1** │ Synthesis scheme of the PSA/SiO₂/Fe₃O₄/AuNPs/lignin microspheres (L-MMS).

Figure 2 │ (a) HRTEM of Fe3O4/AuNPs on the surface of PSA/SiO₂ microsphere; (b) high magnification TEM shows the dispersion of Fe₃O₄/AuNPs on a single microsphere; (c) EDS spectra from the surface of a single microsphere. The scale bars are 300 nm and 10 nm for A and B, respectively.

peak corresponding to N1s was observed at 400.0 eV (Figure S1, Supporting Information, available online at http://www.iwaponline.com/wst/072/399.pdf). Table S1 (online at http://www.iwaponline.com/wst/072/399.pdf) describes the elemental composition during the formation steps of the microspheres as extracted from XPS data. The Fe and Au atomic % confirmed the high packing of both

Fe₃O₄NPs and AuNPs. After the conjugation of lignin in L-MMS, the atomic % of Au and Fe were decreased most likely due to the formation of the lignin layer. The calculated molecular composition closely matched the composition of the starting materials within 5% standard deviation. The magnetic permeability of L-MMS was evaluated by a vibrating sampling magnetometer at room temperature. The

magnetic saturation value was 32.14 ± 0.09 emu g^{-1} (Figure S2, Supporting Information, online at http://www.iwaponline.com/wst/072/399.pdf).

Electrochemical characterization

Subsequently, the electrochemical detection scheme of TNT was constructed by modifying the GCE surface with L-MMS films. Surface modification is used to enhance the sensitivity and selectivity of the electrochemical measurement (Hrapovic *et al.* 2006; Filanovsky *et al.* 2007; Maduraiveeran & Ramaraj 2009; Tang *et al.* 2010; Lu *et al.* 2011; Chen *et al.* 2012). L-MMS was drop-casted onto the electrode surface to form a stable film. Then, the electrochemical response of the system was used to investigate the ability of L-MMS modified GCE to detect TNT in aqueous media. Figure 3(a) and 3(b) show the cyclic voltammograms (CV) of the bare and L-MMS modified GCE in 0.5 M NaCl containing increasing concentrations of TNT at a scan rate of 100 mV/s. In the presence of 50 nM TNT, the bare GCE produced weak and broad reduction peaks at -522, -700, and -824 mV corresponding to the sequential reduction of nitro groups to the corresponding amines (Zhang *et al.* 2006). On the other hand, the L-MMS modified GCE produced well-defined reduction peaks with about a 10-fold increase in peak current and a negative potential shift at the same TNT concentration (Figure 3(b), red curve). The reduction peaks appeared at -541, -724, and -878 mV. When TNT concentration was reduced to 5 nM, the three reduction peaks are still clearly identified with L-MMS modified GCE while they were undetectable in the case of the bare

electrode. Furthermore, the electrochemical response was compared for each preparation step of L-MMS in the presence of 30 nM TNT. A significant enhancement of the reduction peaks were observed for GCE modified with L-MMS as compared with PSA/SiO$_2$/Fe$_3$O$_4$/AuNPs and PSA/SiO$_2$/Fe$_3$O$_4$, respectively (Figure S3, Supporting Information, online at http://www.iwaponline.com/wst/072/399.pdf). The higher sensitivity of L-MMS towards TNT could be explained by: (i) the ability of the lignin modified magnetic nanoparticles to selectively capture and pre-concentrate the target TNT molecules; (ii) the high packing, and the electromagnetic coupling between Fe$_3$O$_4$NPs and AuNPs which enhanced the localized electrochemical reduction of TNT. A typical amperometric (*i-t*) curve was used to further illustrate the detection sensitivity of the L-MMS modified GCE towards TNT. As shown in Figure 4(a), when microlitres of TNT with a concentration range from 0.01–10 nM were spiked into 0.5 NaCl buffer solutions, the oxidation current responded steeply and a steady state was reached. The inset of Figure 4(a) represents a magnification of the first three concentrations of TNT. The electrode response time varies from 5–10 seconds. This excellent sensitivity of the modified electrode could be attributed to the lignin layer and highly packed Fe$_3$O$_4$/AuNPs on the electrode surface. A linear relationship was observed between current response and TNT concentration in the range of 0.05–10 nM (Figure 4(b)). The linear regression equation was {(I) $\mu A = 0.10206 + 0.0077$ (C) nM}, with a sensitivity of 4.81 ± 0.07 μA and a limit of detection (LOD) of 35 pM; $R^2 = 0.9987$. LOD was estimated from $3(S_b/m)$, where S_b is the standard deviation of the
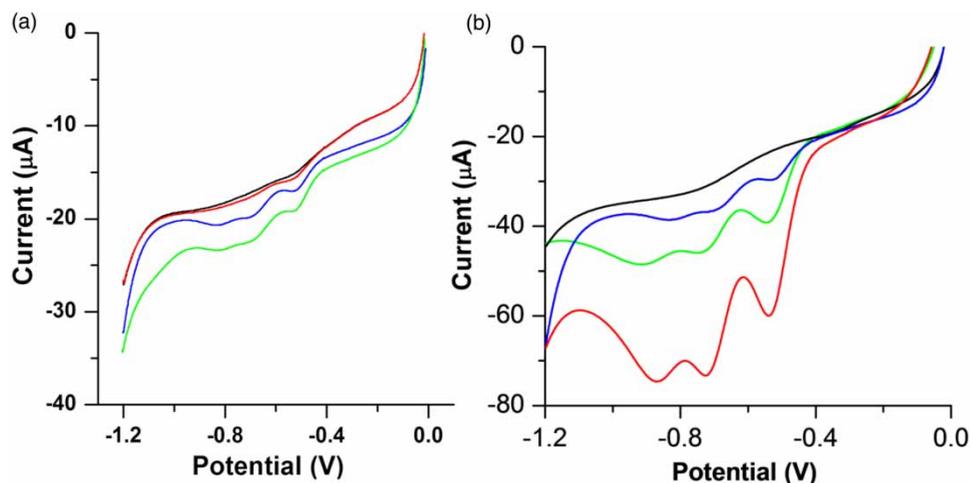

Figure 3 | (a) Cathodic voltammograms for bare glassy carbon electrode (GCE); and (b) L-MMS -modified GCE in 0.5 M NaCl solution containing increasing concentrations of TNT {0 (black), 5 (blue), 30 (green), 50 (red) nM, respectively}.
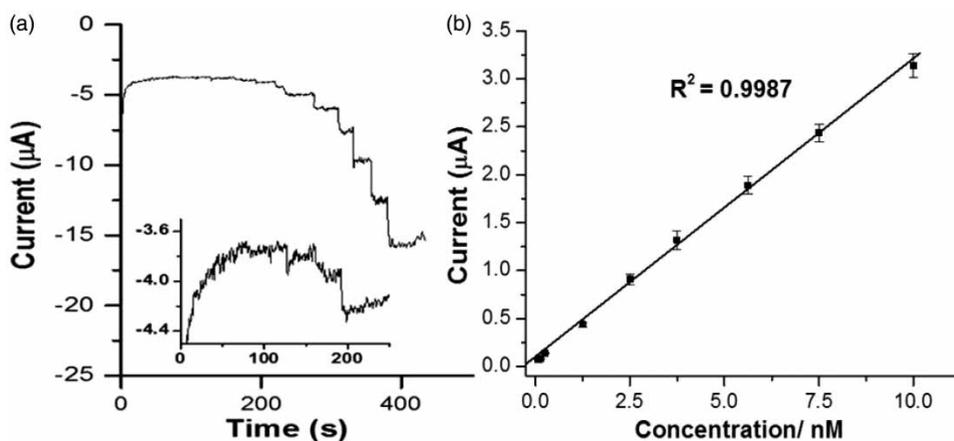
Figure 4 | (a) The current–time (*i-t*) response of L-MMS/GCE measured at −541 mV in 0.5 M NaCl solution with successive additions of 0.01–10 nM TNT; (b) linear relationship between peak current and TNT concentration. Scan rate = 0.1 Vs^{-1}, Pt counter, Ag/AgCl reference electrodes.

measurement signal for the blank and m is the slope of the analytical curve in the linear region. The response signal for 10 nM TNT was 1.8-fold higher than 5 nM. The LOD was significantly lower than values reported using other nanomaterial-modified GC electrodes in the range of 1.5–44 nM (Wang *et al.* 2004; Zhang *et al.* 2006; Fernández *et al.* 2014). The results provide the new hybrid material as a rapid and selective sorbent of TNT. Although a lower detection limit of TNT was obtained previously by surface enhanced Raman scattering (SERS) using L-MMS (Mahmoud & Zourob 2013), electrochemical detection provides a cheaper and more versatile assay for the on-site detection and subsequent remediation of TNT in complex water samples.

Electrochemical detection assay

Next, it was important to evaluate the ability of L-MMS/GCE to detect trace TNT from water samples. Deionized water was used as the reference water source and each experiment was done in triplicate. Figure 5 describes the detection and magnetic separation scheme. Typically, 1 mg of L-MMS is added to water samples spiked with different concentrations of TNT. After the extraction experiment is complete, magnetic separation is used to collect the magnetic microspheres
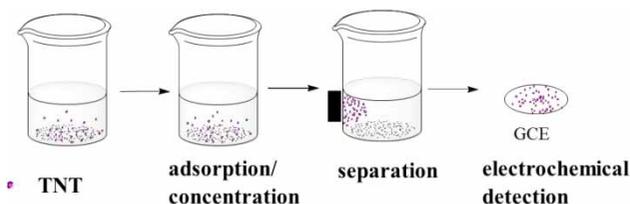

Figure 5 | The detection scheme for TNT from water samples using L-MMS.

bearing TNT. Different TNT-bearing L-MMS/GCEs were evaluated with differential pulse voltammetry (DPV) in 0.5 M NaCl buffer solution using a 3 electrode cell as described in the experimental section. DPV was used in this case because it can provide sensitive detection and diminishes the background current, especially in complex media. Figure 6(a) shows DPV curves with increasing current density corresponding to the increasing initial concentration of TNT. The results from Figure 6(b) reveal that the representative peak current of TNT at −541 mV had a linear relationship with the increase of TNT concentration in the range of 10–400 nM with a sensitivity of 30.2 ± 0.5 μA and an LOD of 1.8 nM; R^2 = 0.9997. The low detection limit could be attributed to the high ability of L-MMS to absorb TNT from complex media, excellent electrochemical activity of L-MMS hybrid material, the large surface area, and the synergistic effect of Fe_3O_4/AuNPs. Total recovery of the initial TNT concentration was 92%, quantified by comparing DPV current signals of the recovered TNT from the water samples with those of the corresponding initial concentrations.

Selectivity and reproducibility of the electrochemical assay

Selectivity of the electrochemical method towards TNT has been tested by comparing the response of L-MMS/GCE to other structure-like analytes. An efficient modified electrode should be able to discriminate the target analyte from common interferences in ambient conditions (Blue *et al.* 2013); 0.1 μM of TNT and structure-like molecules (toluene, DNB, and DNT) were compared following the above described detection scheme. As described in Figure 7(a),
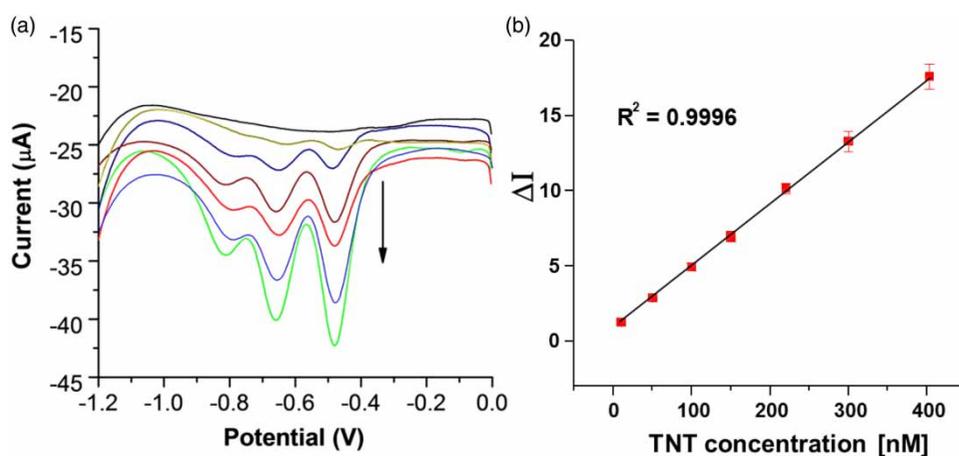
Figure 6 | (a) Differential pulse voltammetry (DPV) for different concentrations of TNT in 0.5 M NaCl on L-MMS /GCE. TNT concentration range: 0–400 nM; (b) linear relationship between peak current ratio and TNT concentration from DPV ($\Delta I = I/I_o$, I, I_o are the current intensity in presence and absence of TNT, respectively).
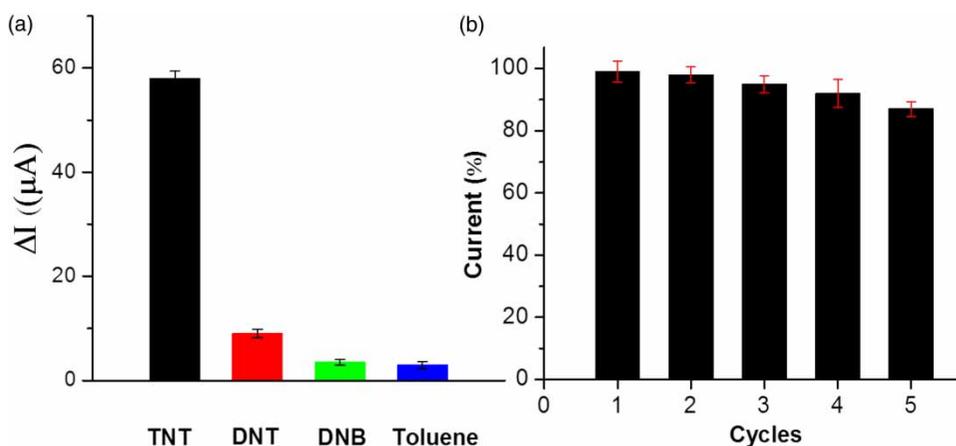

Figure 7 | (a) DPV peak current ratio of L-MMS /GCE in 0.5 M NaCl solution containing 1 μM TNT, DNT, DNB, and Toluene ($\Delta I = I/I_o$, I, I_o are the current intensity in presence and absence of the analyte, respectively); (b) representative current response of L-MMS /GCE after repeated cycles of magnetic separation of TNT and reuse.

TNT showed much higher electrochemical response as compared with toluene, DNB, and DNT. As expected, toluene showed negligible change of current intensity. The slight current enhancement was observed by the addition of DNB, and DNT. Although DNT has the most similar structure to TNT, the electrochemical sensor demonstrated far better selectivity towards TNT as compared with DNT. This is most likely due to the high affinity of the lignin layer to TNT which improved the selective capture and pre-concentration of the TNT molecules on L-MMS/GCE surface and therefore greatly enhanced the electrochemical signal of TNT as compared with structure-like nitroaromatics (Zhang *et al.* 2011; Mahmoud & Zourob 2013). Lignin is known to have a strong adsorption capacity for TNT, at neutral pH, through hydrogen bonding formation (Zhuo *et al.* 2009; Zhang *et al.* 2011). Previous reports indicate that CV

can differentiate explosive compounds such as DNT/TNT from others such as nitrobenzene (Chen *et al.* 2006). Electrochemical detection of nitro-explosives has also been previously demonstrated in environmental samples using mediated electrode systems and exhibited excellent differentiation between differing nitroaromatic species (Chen *et al.* 2006; Guo *et al.* 2011). The reusability of the L-MMS composite was investigated by regenerating the microspheres after desorbing TNT with ethanol (2 ml/mg) for 30 minutes. after each run. More than 88% recovery was obtained after five adsorption/desorption cycles (Figure 7(b)).

TNT detection from real water samples

The electrochemical detection scheme was further investigated in real water samples. Tapwater and seawater

samples were used with salinity 430 ppm and 38,000 ppm, respectively. Under optimum conditions, L-MMS was exposed to the tapwater and seawater samples containing 1 μM of TNT. The recovery assay and electrochemical test were performed as described above in Figure 5. The relative recovery was estimated from the ratio of the DPV signals obtained for 1 μM TNT in real water samples and ultrapure water. The relative recoveries for seawater and tapwater were 96% and 98%, respectively. This insignificant difference of the total recovery and the negligible effect of water salinity have proven the efficiency of the L-MMS to detect TNT in complex water matrices. Selectivity and applicability of sensors to 'real' environmental samples is an important factor in their deployment in field settings. Due to their high selectivity and sensitivity, the electrochemical sensor presented here forms an excellent basis for the quantification of trace TNT in real samples. This was comparable with other electrochemical sensing platforms which have been used for TNT detection, with LOD as low as 1–17 μM in sea, lake or tap water (Guo *et al.* 2011; Caygill *et al.* 2012; Caygill *et al.* 2013).

CONCLUSIONS

The current study presented a simple and selective electrochemical detection method for TNT in water media using lignin-modified magnetic microspheres as an active layer on the GCE. The LOD determined by amperometric *i-t* curve was 35 pM. An excellent catalytic activity of the modified electrode represents response time from one second or less for concentrations above 10 nM to 3 seconds near the detection limit. Also, TNT was successfully detected and removed from both tapwater and seawater with about 96% total recovery without significant impact on the water salinity. The high efficiency of the L-MMS was attributed to the ability of the lignin-modified magnetic microspheres to selectively capture and pre-concentrate the target TNT molecules which can be removed from water with a magnet. This detection scheme can be easily adopted for developing a versatile, cheap, and yet very sensitive portable sensor for TNT detection in waters. The proposed electrochemical assay can be scalable and may provide practical solutions for security and environmental applications.

ACKNOWLEDGEMENTS

REFERENCES

Blue, R., Vobecka, Z., Skabara, P. J. & Uttamchandani, D. 2013 The development of sensors for volatile nitro-containing compounds as models for explosives detection. *Sens. Actuators B: Chem.* **176** (0), 534–542.

Caygill, J. S., Davis, F. & Higson, S. P. J. 2012 Current trends in explosive detection techniques. *Talanta* **88** (0), 14–29.

Caygill, J. S., Collyer, S. D., Holmes, J. L., Davis, F. & Higson, S. P. J. 2013 Disposable screen-printed sensors for the electrochemical detection of TNT and DNT. *Analyst* **138** (1), 346–352.

Chen, J.-C., Shih, J.-L., Liu, C.-H., Kuo, M.-Y. & Zen, J.-M. 2006 Disposable electrochemical sensor for determination of nitroaromatic compounds by a single-run approach. *Anal. Chem.* **78** (11), 3752–3757.

Chen, X., Cheng, X. & Gooding, J. J. 2012 Detection of trace nitroaromatic isomers using indium tin oxide electrodes modified using β-cyclodextrin and silver nanoparticles. *Anal. Chem.* **84** (20), 8557–8563.

Fernández, E., Vidal, L., Iniesta, J., Metters, J., Banks, C. & Canals, A. 2014 Screen-printed electrode-based electrochemical detector coupled with in-situ ionic-liquid-assisted dispersive liquid–liquid microextraction for determination of 2,4,6-trinitrotoluene. *Anal. Bioanal. Chem.* **406** (8), 2197–2204.

Filanovsky, B., Markovsky, B., Bourenko, T., Perkas, N., Persky, R., Gedanken, A. & Aurbach, D. 2007 Carbon electrodes modified with TiO_2/metal nanoparticles and their application for the detection of trinitrotoluene. *Adv. Funct. Mater.* **17**, 1487–1492.

Fu, X., Benson, R. F., Wang, J. & Fries, D. 2005 Remote underwater electrochemical sensing system for detecting explosive residues in the field. *Sens. Actuators B: Chem.* **B106**, 296–301.

Guo, S., Wen, D., Zhai, Y., Dong, S. & Wang, E. 2011 Ionic liquid–graphene hybrid nanosheets as an enhanced material for electrochemical determination of trinitrotoluene. *Biosens. Bioelectron.* **26** (8), 3475–3481.

Hrapovic, S., Majid, E., Liu, Y., Male, K. & Luong, J. H. T. 2006 Metallic nanoparticle – carbon nanotube composites for electrochemical determination of explosive nitroaromatic compounds. *Anal. Chem.* **78**, 5504–5512.

Li, H., Sun, Z. Y., Zhong, W. Y., Hao, N., Xu, D. K. & Chen, H. Y. 2010 Ultrasensitive electrochemical detection for DNA arrays based on silver nanoparticle aggregates. *Anal. Chem.* **82**, 5477–5483.

Li, J.-M., Ma, W.-F., Wei, C., Guo, J., Hu, J. & Wang, C.-C. 2011 Poly (styrene-co-acrylic acid) core and silver nanoparticle/silica shell composite microspheres as high performance surface-enhanced Raman spectroscopy (SERS) substrate and molecular barcode label. *J. Mat. Chem.* **21** (16), 5992–5998.

Liu, G. Z., Luais, E. & Gooding, J. J. 2011 The fabrication of stable gold nanoparticle-modified interfaces for electrochemistry. *Langmuir* **27**, 4176–4183.

Lu, X., Qi, H., Zhang, X., Xue, Z., Jin, J., Zhou, X. & Liu, X. 2011 Highly dispersive Ag nanoparticles on functionalized graphene for an excellent electrochemical sensor of nitroaromatic compounds. *Chem. Commun.* **47**, 12494–12496.

Maduraiveeran, G. & Ramaraj, R. 2009 Potential sensing platform of silver nanoparticles embedded in functionalized silicate shell for nitroaromatic compounds. *Anal. Chem.* **81**, 7552–7560.

Mahmoud, K. A. & Zourob, M. 2013 Fe3o4/Au nanoparticles/ lignin modified microspheres as effectual surface enhanced Raman scattering (SERS) substrates for highly selective and sensitive detection of 2,4,6-trinitrotoluene (TNT). *Analyst* **138** (9), 2712–2719.

McQuade, D. T., Pullen, A. E. & Swager, T. M. 2000 Conjugated polymer-based sensory materials. *Chem. Rev.* **100**, 2537–2574.

O'Mahony, A. M. & Wang, J. 2013 Nanomaterial-based electrochemical detection of explosives: a review of recent developments. *Anal. Methods* **5** (17), 4296–4309.

Prakash, R., Choudhary, R. J., Chandra, L. S. S., Lakshmi, N. & Phase, D. M. 2007 Electrical and magnetic transport properties of Fe_3O_4 thin films on a GaAs (100) substrate. *J. Phys.-Condes. Matter* **19**, 486212.

Robinson, I., Tung, L. D., Maenosono, S., Walti, C. & Thanh, N. T. K. 2010 Synthesis of core-shell gold coated magnetic nanoparticles and their interaction with thiolated DNA. *Nanoscale* **2** (12), 2624–2630.

Stöber, W., Fink, A. & Bohn, E. 1968 Controlled growth of monodispersed spheres in the micron size range. *J. Colloid Interface Sci.* **26** (1), 62–69.

Tang, L., Feng, H., Cheng, J. & Li, J. 2010 Uniform and rich-wrinkled electrophoretic deposited graphene film: a robust electrochemical platform for TNT sensing. *Chem. Commun.* **46**, 5882–5884.

Tenhaeff, W. E., McIntosh, L. D. & Gleason, K. K. 2010 Synthesis of poly (4-vinylpyridine) thin films by Initiated Chemical Vapor Deposition (iCVD) for selective nanotrench-based sensing of nitroaromatics. *Adv. Funct. Mater.* **20**, 1144–1151.

Thomas, S. W., Joly, G. D. & Swager, T. M. 2007 Chemical sensors based on amplifying fluorescent conjugated polymers. *Chem. Rev.* **107**, 1339–1386.

Wang, J., Hocevar, S. B. & Ogorevc, B. 2004 Carbon nanotube-modified glassy carbon electrode for adsorptive stripping voltammetric detection of ultratrace levels of 2,4,6-trinitrotoluene. *Electrochem. Commun.* **6**, 176–179.

Zhang, H. X., Cao, A. M., Hu, J. S., Wan, L. J. & Lee, S. T. 2006 Electrochemical sensor for detecting ultratrace nitroaromatic compounds using mesoporous SiO_2-modified electrode. *Anal. Chem.* **78**, 1967–1971.

Zhang, J., Lin, X., Luo, X., Zhang, C. & Zhu, H. 2011 A modified lignin adsorbent for the removal of 2,4,6-trinitrotoluene. *Chem. Eng. J.* **168** (3), 1055–1063.

Zhou, X. R., Luo, X. G., Lin, X. Y. & Xu, C. G. 2009 Lignin-quaternary adsorbent: synthesis characterization and application for 2,4,6-trinitrotoluene (TNT) adsorption. *Mater. Sci. Forum* **620**, 117–120.

Zhou, H., Zhang, Z., Jiang, C., Guan, G., Zhang, K., Mei, Q., Liu, R. & Wang, S. 2011 Trinitrotoluene explosive lights up ultrahigh Raman scattering of nonresonant molecule on a top-closed silver nanotube array. *Anal. Chem.* **83**, 6913–6917.